Power output variations of co-located offshore wind turbines and wave energy converters in California

Eric D. Stoutenburg [a,*], Nicholas Jenkins [b], Mark Z. Jacobson [a]

[a] Department of Civil and Environmental Engineering, Stanford University, 473 Via Ortega, Stanford, CA 94305, USA
[b] Institute of Energy, Cardiff University, School of Engineering, Cardiff, UK

ABSTRACT

The electric power generation of co-located offshore wind turbines and wave energy converters along the California coast is investigated. Meteorological wind and wave data from the National Buoy Data Center were used to estimate the hourly power output from offshore wind turbines and wave energy converters at the sites of the buoys. The data set from 12 buoys consists of over 1,000,000 h of simultaneous hourly mean wind and wave measurements. At the buoys, offshore wind farms would have capacity factors ranging from 30% to 50%, and wave farms would have capacity factors ranging from 22% to 29%. An analysis of the power output indicates that co-located offshore wind and wave energy farms generate less variable power output than a wind or wave farm operating alone. The reduction in variability results from the low temporal correlation of the resources and occurs on all time scales. Aggregate power from a co-located wind and wave farm achieves reductions in variability equivalent to aggregating power from two offshore wind farms approximately 500 km apart or two wave farms approximately 800 km apart. Combined wind and wave farms in California would have less than 100 h of no power output per year, compared to over 1000 h for offshore wind or over 200 h for wave farms alone. Ten offshore farms of wind, wave, or both modeled in the California power system would have capacity factors during the summer ranging from 21% (all wave) to 36% (all wind) with combined wind and wave farms between 21% and 36%. The capacity credits for these farms range from 16% to 24% with some combined wind and wave farms achieving capacity credits equal to or greater than a 100% wind farm because of their reduction in power output variability.

© 2010 Elsevier Ltd. All rights reserved.

1. Introduction

With solar, wind, and wave energy resources, many coastal areas of the world will be able to use resource diversity to reduce the variability of renewable power and lower the system integration costs of renewables. Combining renewable energy resources with low temporal correlations has been shown to 1) reduce the aggregate power output variability of renewables [1–13], 2) reduce the operational requirement for reserve and regulating power [14–18], and 3) reduce the requirement for generation capacity to maintain power system reliability [1,2,5,17,19–21]. This study assesses the potential of co-locating offshore wind turbines and wave energy converters at offshore locations in California where both resources are abundant and examines the benefits for the electric power system. It builds on several previous studies [22–26] by examining specifically co-located wind and wave energy farms,

modeling the reduced variability in California's electric power system, and extending the methodology of aggregating power from geographically diverse wind farms to wave farms.

California's offshore wind resource is high [27,28], but currently remains undeveloped because of the deep water off California's coast. However, deep water floating wind turbines that can access this vast resource are being developed [29,30]. Similarly, California has a good wave energy resource especially in the north [31], and a few wave energy converters are being tested in real sea conditions [32,33]. It is possible that both technologies will achieve commercial status on similar timelines and can be co-located. Their aggregate power output is significantly less variable than are individual technologies and can support California's efforts to increase the penetration of renewables into the electric power system.

2. Methodology

To explore the benefits to the electricity system, the power output from farms of V90 Vestas 3.0 MW offshore wind turbines

---

* Corresponding author. Tel.: +1 650 721 2650; fax: +1 650 723 7058.
E-mail address: estout@stanford.edu (E.D. Stoutenburg).

and 750 kW Pelamis Wave Energy Converters was calculated using wind and wave data collected from buoys at 20 locations. The use of buoy data allows the power output of a wind turbine and wave energy converter located at the same location in the Pacific Ocean, in real sea conditions, to be estimated since the buoy contains instruments to measure wind speed and wave parameters simultaneously.

The hourly time series of power output from each energy source and buoy location is then examined to determine power performance, reductions in variability on several time scales, and correlations between resources and locations. The requirement for load following reserves is estimated by combining the hourly load variations and the hourly ramp rates of renewables added to the power system. The power output is simulated in a simple model of the California electricity system to examine the impacts on system reliability [34–36] and derive the capacity credit of each renewable [2,3,5,7,37]. The following sections detail the methodology used in this study.

2.1. Data source: national data buoy center buoys

The US National Oceanic and Atmospheric Administration's National Data Buoy Center (NDBC) maintains an extensive buoy system to collect meteorological and oceanographic measurements [38]. There are 20 buoys with both wind and wave data in the historical record for California from 1980 to 2008, 17 of which were still operational as of December 2008. Two buoys were eliminated from the study because they were over 50 miles offshore, leaving 18 for analysis. The NDBC gives each buoy a 5 digit identification number. All California buoys operated by the NDBC are numbered 460XX, so for this study only the last 2 digits are used as an identifier, e.g. buoy 46054 near Santa Barbara is simply buoy 54. The buoys have 5–28 years in their record. The harsh operating conditions offshore and maintenance service leaves missing data in the records. Linear interpolation of the wind speed with the $i-1$ and $i+1$ h is used if 1 h of data, hour i, is missing. Longer periods of missing data were not reconstructed. The wave resource is less variable, so linear interpolation of missing data was used up to 5 consecutive hours. Missing data beyond 5 h were not reconstructed. No annual record with more than 5 days of missing data from any month (120 h; 16%) was used for the analysis. This ensures only annual records with data representative of the entire year were used to account for the highly seasonal nature of the wind and wave resource. There were 143 annual records constituting over 1,000,000 h of wind and wave data collected simultaneously that met this data quality criteria.

2.2. Wind power

The NDBC buoys report hourly mean wind speeds at 5 m above sea level for most buoys [39]. Wind speed was extrapolated to the hub height at 80 m using the logarithmic law assuming neutral atmospheric stability conditions [40]. The neutral assumption is conservative and likely underestimates wind speed, since the atmosphere is usually stable over the Pacific Ocean off California and wind speeds are usually higher than predicted with the logarithmic law as noted in [41]. Vestas' published power curve was used to calculate the electric power output of a single wind turbine. The smoothing effect of multiple turbines in a farm was captured using a multi-turbine power curve that adjusts the power output from a single turbine to account for the distribution of wind speeds expected in a wind farm based on a single point measurement of the wind speed in the farm [42].

2.3. Wave power

The NDBC buoys have accelerometers that measure wave motion and a fast Fourier transform algorithm calculates hourly significant wave height and dominant (peak) wave period [43]. These two parameters were used to calculate the power output of the Pelamis Wave Energy Converter using the methodology of [44]. This two parameter estimation of the power output of the wave energy converters assumes a Pierson-Moskowitz wave spectrum [33]. This spectrum applies for a fully developed sea where the winds and waves achieve a long time, long fetch equilibrium, which should more closely approximate the spectrum of the Pacific Ocean compared to other model spectrums like JONSWAP [45].

2.4. Farm aggregate power

Aggregate power for the offshore energy farms with wind and wave was constructed on a capacity basis in MW. A 500 MW farm with 50% wind and 50% wave will therefore have 250 MW installed capacity of each. Rotor wake losses for offshore wind farms are estimated at 6–20% of total power [46,47]. This study assumes 10% wake losses for the wind turbine array although innovative farm layout with wind and wave energy converters may permit increased spacing between the turbines consequentially lowering the wake losses.

The extent to which wave diffraction and reflected waves from very large arrays of these wave energy converters results in a similar wake loss type effect is uncertain. Depending on the array layout, regions of constructive and destructive wave interference will exist that will increase or decrease the power output from individual converters [48]. This study assumed no power losses from wave energy converter interactions or from wind turbine towers affecting the wave field. Electrical losses from collection and transmission to shore for a 500 MW offshore wind farm have been estimated at 10–17 MW or 2–3% [49]. An electrical loss of 3% is applied to the aggregate farm for all generation mixes of wind and wave under the assumption that wave energy farms will have comparable electrical losses. Five generation mixes are tested for each offshore farm: 1) 100% wind, 2) 75% wind and 25% wave, 3) 50% wind and 50% wave, 4) 25% wind and 75% wave, and 5) 100% wave.

2.5. Power statistics, geographic and resource correlations

Using the methodology described in Sections 2.2–2.4, the power output for an offshore wind farm, wave farm, or combined farm was estimated using data from the 18 buoys off California. Six buoys were eliminated from further study because of a low wind resource (under 30% capacity factor) or a low wave resource (under 20% capacity factor). This leaves 12 potential farms located at buoys with a good wind and wave resource mapped in Fig. 1. These 12 buoys have a total of 93 quality annual records. The capacity factor for wind and wave at each potential farm was calculated as well as their inter-annual, monthly, diurnal, and hourly variability. In this study only power delivered to the grid after farm losses is reported. For example, after wake (−10%) and electrical (−3%) losses a wind farm will deliver to the grid only 87% of the gross energy generated.

Variability in the hourly power output annual time series was analyzed using a histogram of the hourly power output. The correlation between wind and wave, wind and wind at other farms, and wave and wave at other farms was calculated using the Pearson product–moment correlation coefficient, r. The correlations between wind and wave indicate the potential of resource diversity to reduce variability, while the correlations between sites indicate the potential of geographic diversity to reduce variability [2–5,8,17].
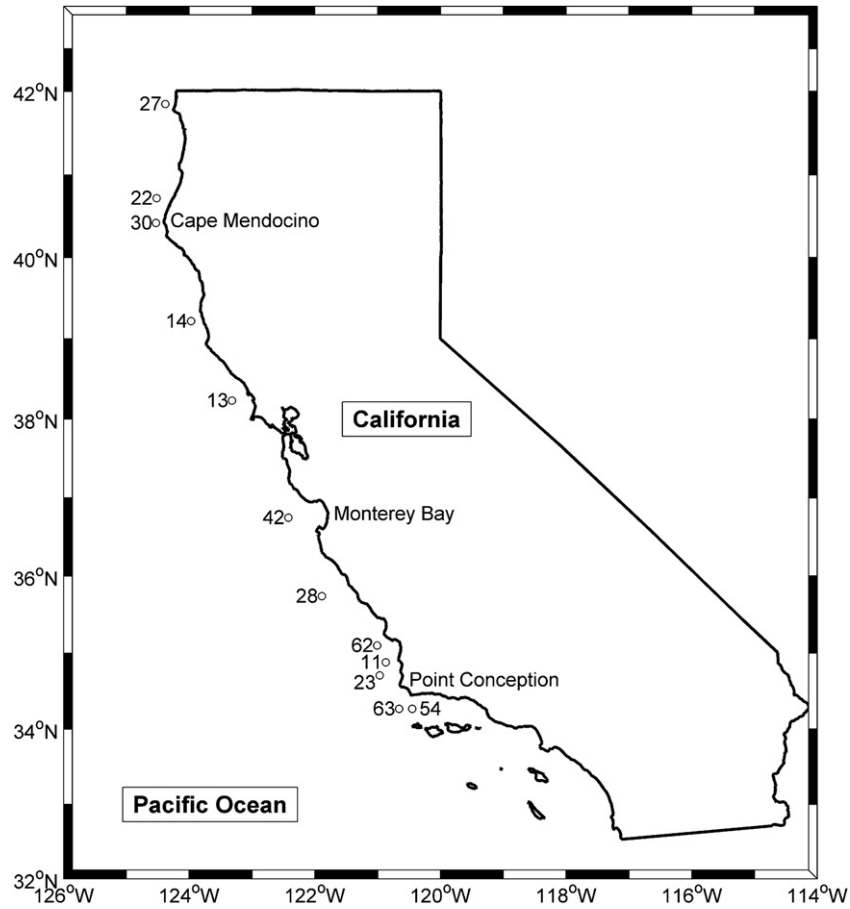
Fig. 1. Map of NDBC buoys collecting wind and wave measurements off the California coast from 1982 to 2008 used in this study.

2.6. System operation: hourly ramp rates and load following reserve requirement

The impact of marine renewables on power system operation and increased load following reserve requirement was calculated with the hourly means of wind power, wave power, and load in California. Hourly resolution of power output and load is of high enough resolution to estimate the requirement for load following reserves [17,50]. The hourly ramp rates and load following reserve requirement was calculated as follows. Net load is the load minus the renewable power generation as in equation (1) and is the load the rest of the generation system must balance.

$$\text{Net Load}_i = \text{Load}_i - \text{Renewables}_i \qquad (1)$$

Hourly ramp rates for the thermal plants with variable renewables in the system are determined by taking the hourly difference of the net load, as in equation (2).

$$\text{Net Load Ramp Rate}_i = (\text{Load}_i - \text{Load}_{i-1}) - (\text{Renewables}_i - \text{Renewables}_{i-1}) \qquad (2)$$

The variability of the net load ramp rates measured as the standard deviation σ can be compared with the load variability without renewables [17,18]. The increase, I, in three standard deviations between net load and load hourly variations is the increased requirement for load following reserves in the system from adding wind power [18]. This is shown in equation (3).

$$I = 3(\sigma_{\text{Net Load}} - \sigma_{\text{Load}}) \qquad (3)$$

2.7. System reliability: loss of load expectation and capacity credit

A generation system adequacy model can indicate the effect of variable renewable energy plants on the electric grid when they are modeled as multistate power plants [21,34–36]. Combined with load data, system reliability indices can be calculated. These indices quantify the expectation of load demand exceeding generation capacity [34]. The model removes conventional thermal plants after adding renewables, which shows the equivalent capacity credit of the renewable plant, while maintaining the same level of system reliability [3,5,7,21,34–37].

California uses a reliability standard of one summer day in ten years where generation fails to meet demand. This is equivalent to a loss of load expectation (LOLE) of 0.1 (one tenth of a day per year) or 2.4 h per year. A simplified model was created for California with all combined cycle natural gas plants (CCGT) of 100 and 200 MW and various wind and wave energy farms as in Fig. 2. Although California has a more diverse generation mix with nuclear and hydropower, the modeled system closely matched the actual existing generation capacity with the LOLE = 0.1 [51]. Forced outage rates for CCGT plants from the North American Electric Reliability Corporation Generation Availability Data System [52] were used and renewable plants were modeled with their multistate power output following the methodology in [35].
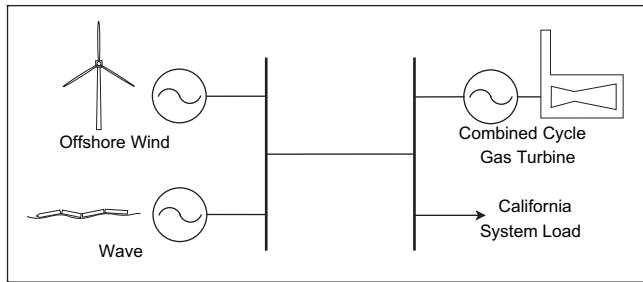
Fig. 2. Simplified California generation system model.

Table 1
Average annual capacity factors and relative rankings of wind and wave energy at 12 NDBC buoys.

Buoy Number	Buoy Name	Capacity Factors		Rankings		Coastline
		Wind	Wave	Wind	Wave	
27	St Georges	0.30	0.27	12	4	north of point
22	Eel River	0.30	0.29	11	1	north of point
30	Blunts Reef	0.41	0.28	3	3	at point
14	Pt Arena	0.33	0.29	8	2	parallel coast
13	Bodega Bay	0.38	0.25	5	6	parallel coast
42	Monterey	0.32	0.25	9	7	mouth of bay
28	Cape San Martin	0.38	0.26	6	5	parallel coast
62	Pt. San Luis	0.36	0.22	7	11	south of point
11	Santa Maria	0.32	0.23	10	10	north of sharp point
23	Pt. Arguello	0.38	0.24	4	9	north of sharp point
63	Pt. Conception	0.46	0.24	2	8	south of sharp point
54	Santa Barbara	0.50	0.22	1	12	south of sharp point

The California Independent System Operator (CAISO) conducts a Summer Loads and Resources Operations Preparedness Assessment annually to assess the capability of the power system to meet the summer peak loads [53]. This study follows that approach and uses the California hourly load data reported by the CAISO between June 15 and September 15 for 2001 [54] as the statistical hourly load demand for the summer period (peak CA demand season). Ten 500 MW wind and/or wave energy farms were modeled at the ten buoys with quality annual records for 2001. The year 2001 is chosen because that year has the most buoys to represent the resources across the state. Five GW of renewables is sufficiently large to show system reliability impacts as the state approaches its 20% renewable portfolio standard goal.

3. Results and discussion

3.1. Power statistics, geographic and resource correlations

3.1.1. Capacity factors

Table 1 shows the annual average capacity factors for a modeled wind or wave energy farm at each buoy. Wind has higher average capacity factors than wave has. As wave energy converter designs advance, higher capacity factors may be expected. The wave energy converter used in this study is optimized for the shorter wave period climate of the Atlantic Ocean than the Pacific Ocean with longer period swells.

The relative rankings of the buoy's capacity factors can be explained by observations of the wind and wave resource. Winds are driven by the seasonal position and intensity of the semi-permanent Pacific high and Aleutian low. This creates the predominant winds out of the north and northwest. During the winter, the passage of a cold front can create strong winds that can be directionally variable from the west and south. The buoys with the highest wind power are located at or near capes and points

along the coast, where fan expansion accelerates winds in the marine boundary layer especially during the summer [27]. The one outlier at Point Arguello, buoy 23, is better explained by its far distance offshore (30 km) compared to nearby buoys. The coast from Los Angeles to San Diego has no significant wind energy resource since Point Conception shields it from the strong northwesterly winds flowing down the coast.

Wave energy increases with latitude along the California coast [31] and potential farms with the highest wave energy are north of San Francisco. The Aleutian low pressure system sends northwest wave trains toward California that refract and become parallel to the coast as they approach it. For this reason in all seasons, the hourly mean wave direction is generally from the west-northwest and parts of the coast that face northwest have the highest incident wave energy, as buoy 22 demonstrates. During the summer, some southern wave swells generated by tropical storms further south reach California, but that contribution to a site's wave energy is not significant averaged over a year. As with wind, there is little wave resource south of Point Conception near the coast because of the sharp refraction of Point Conception and shadowing by the Channel Islands. All the buoys are in deep enough water that the water depth does not significantly affect the waves [55].

Those general observations about the wind and wave energy resource confirmed by the buoy data allow an exploration of the possible siting and configurations of offshore wind and wave energy farms. The likely locations for combining the resources are at points and capes shown in Fig. 3. At points, the incident wave energy approaches from the northwest while the northwest winds accelerate around the point. The ideal region for wind is just south of the point and for wave it is just north of the
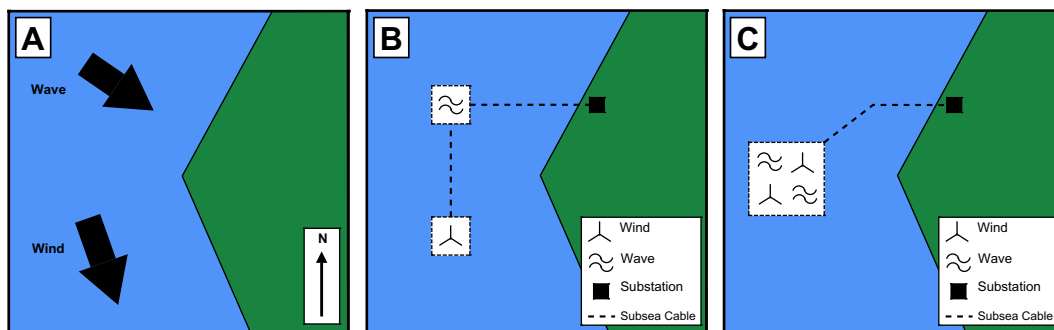

Fig. 3. Schematic diagram of potential co-located offshore wind and wave energy farm configurations. Diagram A: predominant wind and wave direction; arrows placed at regions of highest resource. Diagram B: shared subsea shore-linked transmission cable system of separate but close proximity offshore wind and wave energy farms. Diagram C: innovative co-located wind and wave energy farm.
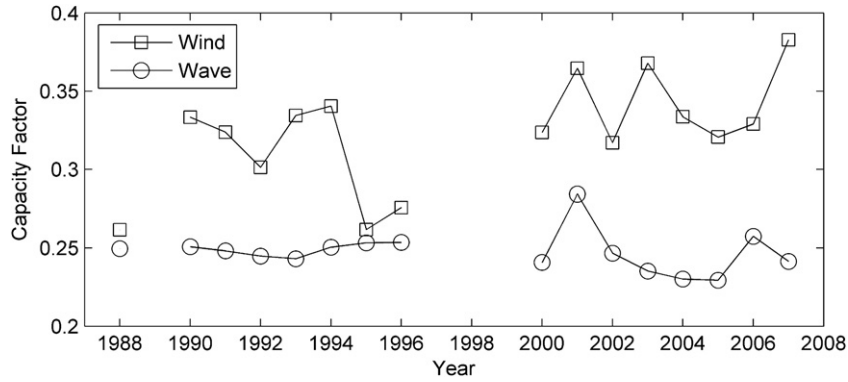
Fig. 4. Annual wind and wave capacity factors of the NDBC buoy with the longest quality record, 16 years, Buoy 42 in Monterey Bay.

point. This could lead to an array of wind turbines (WT) to the south and an array of wave energy converters (WEC) to the north connected and sharing a common subsea transmission cable(s) to shore. An innovative configuration to increase the energy density extracted per square kilometer of ocean would be co-located arrays of WTs and WECs at the point where both resources are high at the point or cape. In areas with competing sea space uses or limited areas for permitting, this may be an attractive configuration.

These possible configurations are supported by the buoy data. The best wind capacity factors are south of Point Conception at buoys 54 and 63. The best wave resource is buoy 22 north of Cape Mendocino near Eureka with a northwest facing coast. The third best wind and third best wave resource is co-located at the only buoy located directly at a point, Cape Mendocino, buoy 30. The steep, rocky terrain and location of terrestrial substations is likely to drive the cable route either north or south of the point to beaches, harbors and infrastructure such as Humboldt Bay north of Cape Mendocino. The buoy near Port Orford, Oregon off Cape Blanco is similarly positioned as buoy 30 is off Cape Mendocino and was also analyzed. It exhibited the same high resource of both wind and wave energy.

3.1.2. Inter-annual variability

Long term climatic variability of wind and wave power output is important for power system planning studies. The inter-annual variability of wind and wave power capacity factors of buoy 42 at Monterey Bay with the longest quality record, 16 years, of any buoy is shown in Fig. 4. Inter-annual variability of wind power is greater than wave power. The standard deviation divided by the mean for wind is 10.8% and wave is 5.1%. The lower annual variation of wave power and generation mixes with wave power would reduce the uncertainty in the energy supply for long range generation adequacy studies.

3.1.3. Seasonal variability

Fig. 5 shows the monthly maximum, mean, and minimum capacity factors of buoy 14 using 11 years of data. These are representative of most of the California buoys. Monthly capacity factors for wind power peak in June and for wave power in December. Both resources experience low monthly capacity factors in the late summer with wind in September and wave in August. Wind power has significant variability in June and December, and wave power in February. Wind power is significantly more variable year to year than wave and any given year generally does not follow
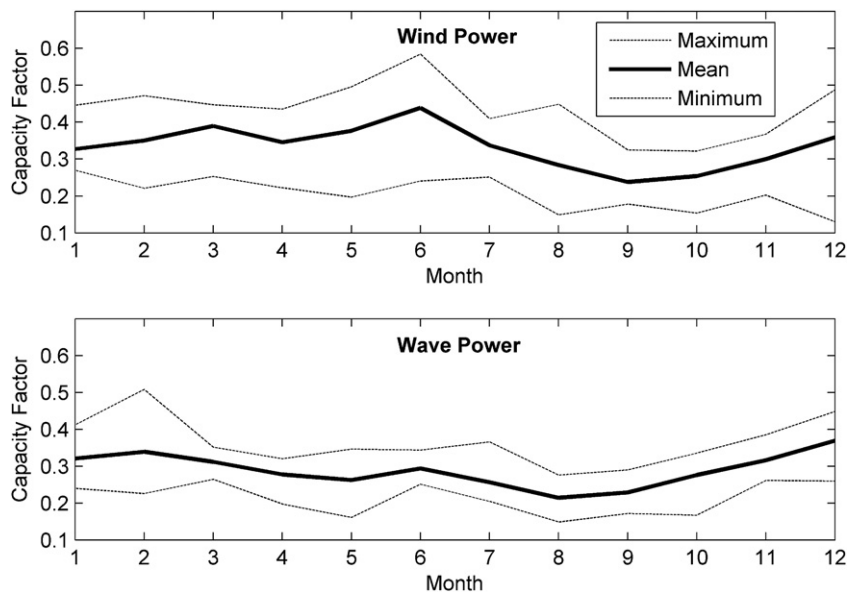

Fig. 5. Monthly capacity factors of wind and wave energy for a representative buoy, buoy 14 at Port Arena.
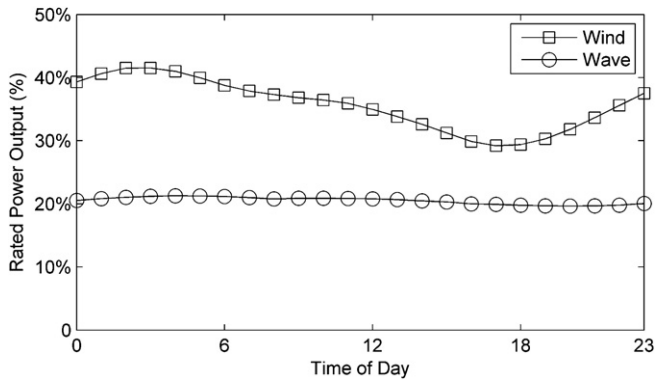
Fig. 6. Average rated power output for an offshore wind farm or wave farm for each hour of the day for the summer months for all buoys and all years with quality annual records.

the long term climatic mean shown in Fig. 5. Individual years for wave power follow the pattern fairly closely with a slow decrease in wave energy from winter to late summer.

3.1.4. Diurnal variability

California's summer peak electricity demand season is from June 15th to September 15th [53]. The diurnal pattern of wind and wave power for this summer season is shown in Fig. 6. This is the average power output for all buoys and all years for wind and wave. Wind power production peaks around 3:00 and declines to its minimum around 17:00 when electricity demand is highest. Wave power generates its power on average evenly throughout all hours of the day during the summer. The use of these diurnal hourly averaged power outputs are used to show the relationship between daily load profiles and renewable power generation [6,8]. However, the conclusions drawn from these diurnal power output profiles are limited, since electric power systems balance generation and load instantly, not *on average*. Since very few summer days actually look like the average power output profile shown in Fig. 6, it is more important to look at the hourly variability of each resource.

3.1.5. Hourly power output variability

The histogram of hourly average power output as a percentage of rated power in Fig. 7 shows the distribution of power output states of buoy 30 for one year. The frequency of low wind speeds and the cut-in and cut-out wind speeds of the wind turbines

produce significant hours of no wind power. The rated wind speed and constant power output from 15 m/s to 25 m/s contribute to the high number of hours at full power for wind. Wave power generation reflects the distribution of the resource better and is approximately a Rayleigh distribution with few hours at full power. The reduction of hours at no power stems primarily from an equivalent low "cut-in" wave height and period and from the consistency of the wave resource. Calm seas in the world's largest ocean basin are rare since wave trains can approach from many directions and a storm system generating waves is always present somewhere.

Fig. 8 shows the histogram of power output for various generation mixes of a farm with both wind and wave for the same one year. There is a significant reduction in hours of no power and full power for the wind and wave energy farms. The number of no power hours (0%–2.5% power where the farm is likely to be exporting little if any power to the grid) reduces to only 70 h for a generation mix of 25% wind and 75% wave, down from 1330 h of no power for a 100% wind farm and 242 h of no power for a 100% wave farm. This indicates that most of the hours with no power for one resource do not occur simultaneously with the other resource. Similarly, hours of full power (after wake loss and electrical losses) drop significantly for the generation mixes. Wind power has 1080 h of full power, wave 44 h, and the generation mix of 25% wind 75% wave has the lowest with 25 h of full power. These results from one buoy, number 30 off Cape Mendocino, are representative of all the buoys in the study.

3.1.6. Correlations: geographic and resource diversity

Reducing variability can be achieved by aggregating power from geographically diverse wind farms [4,8,56] or aggregating power from diverse resources such as wind and wave [22]. A low or negative correlation coefficient (Pearson's) serves as an accessible metric of reduced variability of aggregating two sites or two resources. The correlation matrix in Fig. 9 shows the correlations for geographic and resource diversity. The correlations are between identical hours of the power output of two locations and/or two resources for 193 pairs of annual time series.

The correlation matrix has four sections with buoys sorted from north to south. The upper left section maps the distance between buoys. The upper right and lower left sections are the correlations between wave power at one buoy and wave power at another buoy and wind power at one buoy and wind power at another buoy, respectively. Those two sections examine geographic diversity.
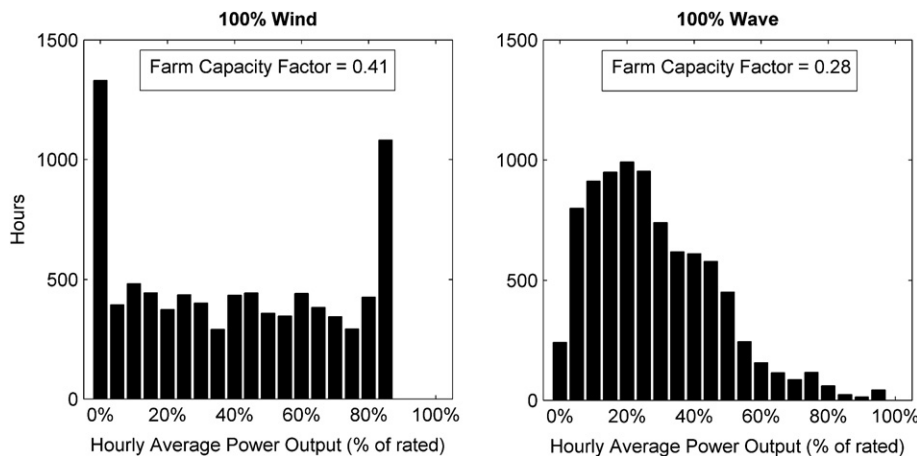

Fig. 7. Histogram of hourly average power output as a percentage of rated power of a 100% wind or 100% wave energy farm at buoy 30 off Cape Mendocino (delivered power after losses).
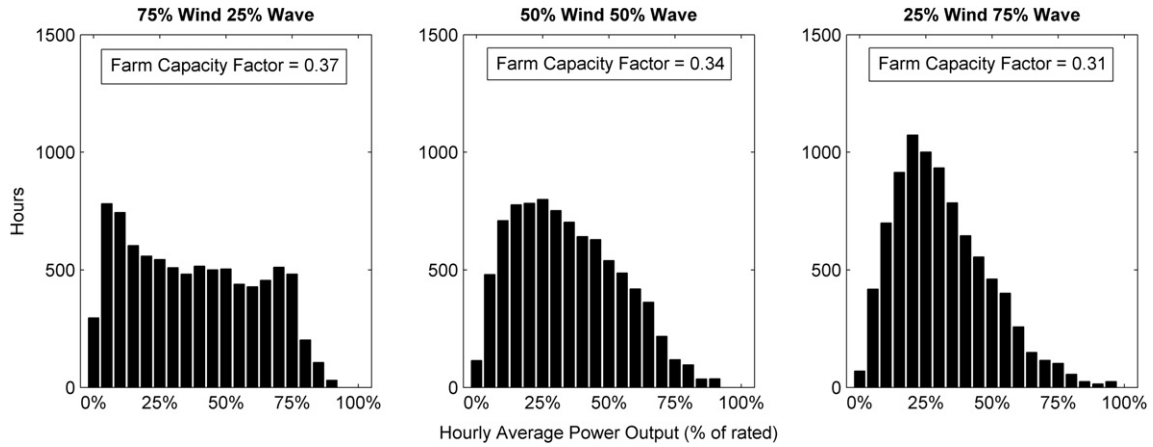
Fig. 8. Histogram of hourly average power output as a percentage of rated power for three mixes of combined wind and wave energy farms at buoy 30 off Cape Mendocino (delivered power after losses).

There is an inverse relationship between distance and correlation. For the same distance between buoys, wind power has a lower correlation than wave power, so less distance is required between offshore wind farms to reduce aggregate power variability. Therefore, the benefits from geographic diversity are greater for wind power than for wave power as expected from the large spatial coherence of the wave resource compared to the wind resource.

The lower right section consists of the correlations between wind power and wave power at the same and different buoys. The diagonal line was drawn on correlations between wind power and wave power at the same buoy. This shows the potential of resource diversity to reduce variability, and the low correlations are comparable with correlations between distant wind or wave power

farms. For example, the correlation between wind and wave power at buoy 30 near Cape Mendocino is 0.29. To achieve the same correlation of 0.29, wind farms at buoys 13 and 54, 520 km apart, or wave farms at buoys 27 and 62, 800 km apart, would need to be connected to the grid. This may imply lower offshore transmission cable costs and transmission upgrades to connect one low variability offshore farm compared to two high variability offshore farms.

In the lower right section above the diagonal are correlations between wind power at a northern buoy and wave power at a southern buoy. Below the diagonal are correlations between wave power at a northern buoy and wind power at a southern buoy. The highest wind-wave correlation, r, was 0.54 between wind at buoy
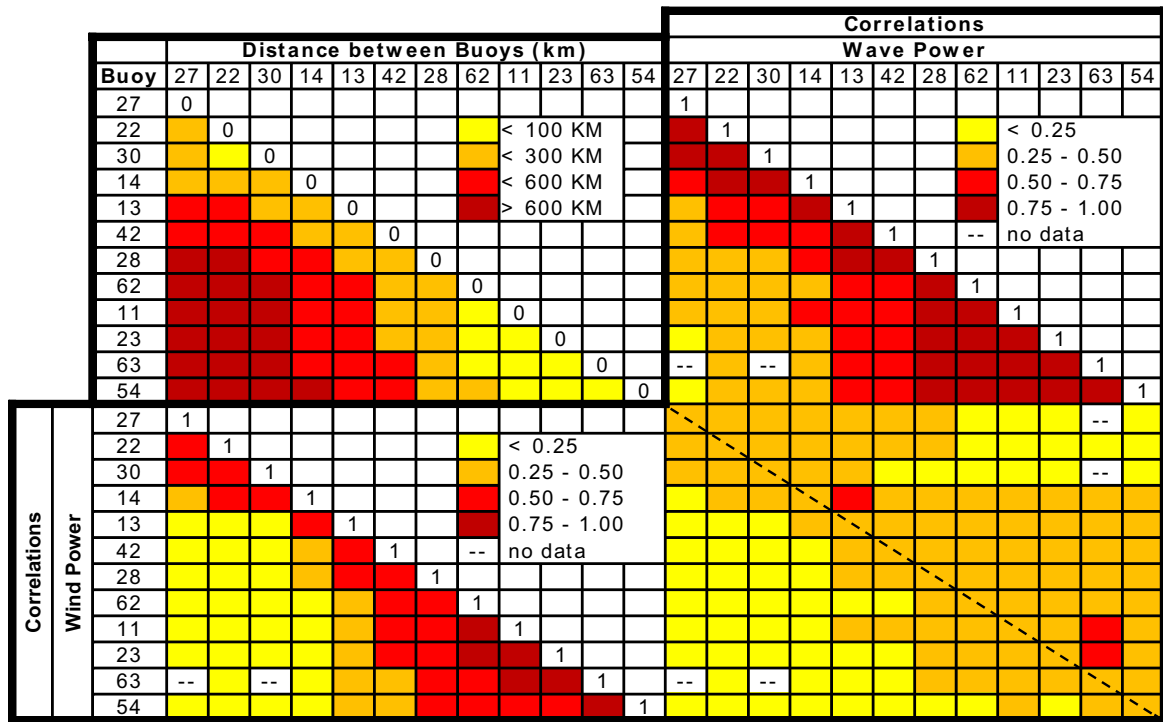

Fig. 9. Correlation and distance matrix for all combinations of buoys and wind and wave power. Upper left section is the distance between buoys. Upper right section is the geographic correlation of wave power between buoys. Lower left section is the geographic correlation of wind power between buoys. Lower right section is the wind-wave resource correlation between the same (diagonal) and different buoys.
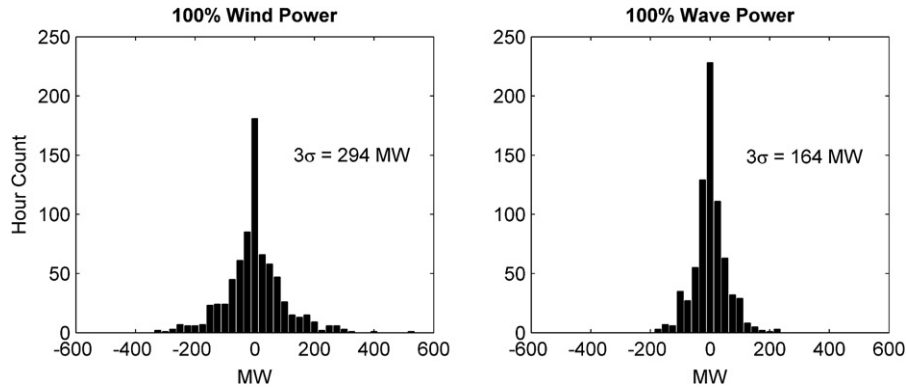
Fig. 10. Farm hourly power output variations, or ramp rates, for 100% wind and 100% wave energy farm of 1000 MW at buoy 30 during the summer of 2001.

14 (north) and wave at buoy 13 (south). The next two highest, also in red in Fig. 9, are wave at buoy 63 with wind at buoy 23 ($r = 0.52$) and with wind at buoy 11 ($r = 0.51$). These are higher than any wind-wave correlation at the same buoy. Higher correlations exist above the diagonal for wind power at a northern buoy and wave power at a southern buoy, than wave power at the same northern buoy and wind power at the same southern buoy. With both resources coming from the northwest direction this can only be explained by what is also observed meteorologically that high wave conditions can precede storm systems. If the storm is at the northern buoy with high winds, then high waves have preceded the high winds and exist at the southern buoy in front of the storm.

3.2. System operation: hourly ramp rates and load following reserve requirement

The power statistics and correlations presented in Section 3.1 consider only the power generation of wind and wave, so it is important to put the modeled power output within the context of the California electricity system, a large, interconnected grid with a peak demand of around 50 GW. The hourly power output variations of a modeled 1000 MW farm at buoy 30 for the summer of 2001 are shown for a 100% wind and 100% wave farm in Fig. 10. Assuming a normal distribution, 3 times the standard deviation would cover 99% of the variations. Wave energy has smaller variations, a function of the resource.

The variations at the farm do not have to be balanced by the system, but instead the net variations, which are the combined load and farm variations. These net load variations represent the hourly ramp rates expected of the other plants in the system in 1 h. The difference in the ±3 σ of the variations of the net load and the load without renewables indicates the expected load following reserves capacity increase [18]. The results of this method are shown in Fig. 11 for a 100% wind and a 100% wave farm of 1000 MW located at buoy 30 with load data during the summer of 2001. The variations of the 100% wind farm are larger than the 100% wave farm, but combine with the load variations such that the increased load following reserve requirement is only 9.4 MW compared to the 100% wave farm requiring 15.2 MW of reserves.

Farms with generation mixes of wind and wave, shown in Table 2, generally improve over farms with only one resource. The least variable farm is 25% wind and 75% wave, a likely choice for an isolated grid. The lowest reserve requirement is the 75% wind and 25% wave farm when considering the net load variations for the California system using the year 2001 load data.

3.3. System reliability: loss of load expectation and capacity credit

The generation capacity adequacy model described in Section 2.7 was used with six power output states. At least a five power output state model has been shown to provide a robust result [35] and that forced outage rates of wind turbines [35] and wave power converters can be ignored relative to the variability in their power output. The probability of an aggregate rated power output state of 0%, 20%, 40%, 60%, 80% or 100% is shown in Fig. 12 for 10 modeled 500 MW farms of wind and/or wave for the summer of 2001. The
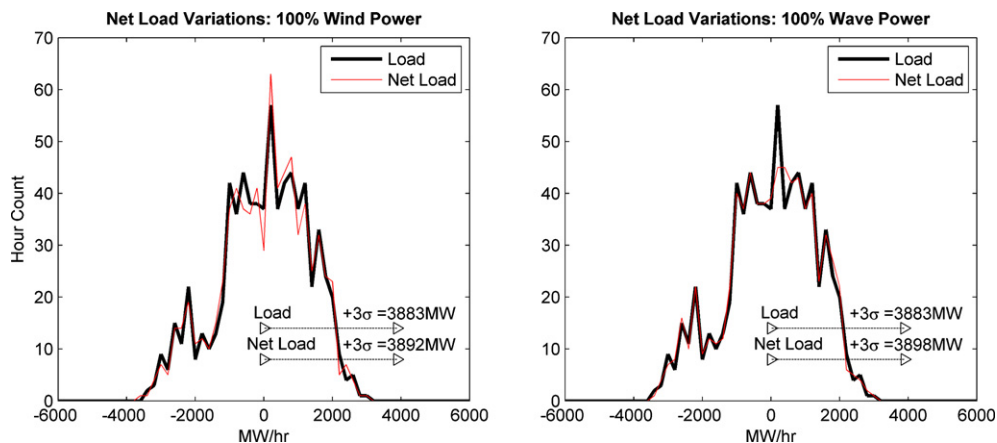

Fig. 11. Load and net load hourly variations for 100% wind and 100% wave energy farms of 1000 MW at buoy 30 combined with summer of 2001 California load data with 3 standard deviations of the variations shown.

Table 2
Three standard deviations of the farm hourly power output variations and the increased load following reserve requirement for the California system with a 1000 MW farm with various generation mixes at buoy 30 during the summer of 2001.

Year	100% Wind	75%–25%	50%–50%	25%–75%	100% Wave
2001	Farm Hourly Variations: $\pm 3\ \sigma$ (MW)				
	294	223	167	142	164
2001	I, Increased Load Following Reserve Requirement (MW)				
	9.4	8.0	8.6	11.0	15.2

probability charts show 100% wind has the highest probability for 80% power output compared to the other generation mixes, while 100% wave has the highest probability for 20% power output. The generation mixes with wind and wave have a lower probability of no power hours than either resource alone.

The six power output states and their associated probabilities were modeled as multistate plants in the California system. Once the marine renewables are added, 100 MW CCGT plants are removed from the system shown in Fig. 2 while maintaining a LOLE no greater than 0.1 day/year or 2.4 h/year. The capacity of CCGT plants removed from the system is the equivalent capacity credit of the marine renewables. The removal of 100 MW plants limits the resolution of the capacity credit calculation. The results for the five generation mixes are presented in Table 3.

In [7], capacity credit is shown to be influenced by three factors: 1) The correlation between renewable power output and demand peaks. This was shown in Table 2 to be similarly negative for wind, wave, and the combinations. 2) The renewables' average power output. Wind and wave capacity factors were shown by example in Fig. 5 (seasonal) and Fig. 6 (diurnal). 3) The range of renewable power output. This was shown in Figs. 7 and 8 for the range in hourly power output of wind, wave, and combinations. The capacity credit can at most equal the capacity factor. This means factor 2 sets the capacity credit limit, and factors 1 and 3 determine the difference between the capacity factor and capacity credit.

The 100% wind case has the highest capacity factor of 36%, but the greatest variance, and has a capacity credit of 24% with a LOLE of 2.09. The capacity credit of wave is the lowest because it has the lowest capacity factor. However, the lower variance of the combinations decreases the difference between the capacity factor and the capacity credit showing the influence of improving the capacity credit from reduced variability. The 75% wind 25% wave mix has a capacity factor of 33%, the same capacity credit as wind of 24%, and the lowest LOLE of 2.02. This means the generation mix of 75% wind and 25% wave contributes most to system reliability of any of the generation mixes. Additionally, the 25% wind and 75% wave mix displaces almost as much generation capacity (capacity credit 22%) as it does energy (capacity factor 25%) in the California power

system, which would reduce the system integration cost as described in [7].

3.4. Discussion

Four insights can be drawn for co-locating wind and wave energy. First, the capacity factors of wind and wave at the 12 buoys indicates where co-located wind and wave energy farms would best be located – at capes and points along the coast where regions of high resource for each renewable overlap. This was best shown by buoy 30 at Cape Mendocino having the third highest wind and third highest wave energy resource. Second, inter-annual variability can be reduced by adding wave energy to offshore wind farms, a significantly less variable resource on this, and all time scales. Both resources have coincident annual lows in the late summer period, but wind peaks generally in the late spring and early summer while wave peaks in the winter, so generation mixes will share the resource peaks over a six month period. Third, the significant reduction in hours of no power show that co-located wind and wave energy farms will almost always deliver some power to the grid. Fourth, the correlations of geographic and resource diversity indicate that combined wind and wave farms will have low correlations comparable with geographically distant wind farms or wave farms, but they achieve this low correlation and corresponding reduction in variability before their interconnection to the grid.

In Section 3.2.1, it was shown that the generation mixes outperform either wind or wave alone using the conventional metrics for load following reserve requirements. The generation adequacy model in Section 3.3 used to calculate the LOLE and resulting capacity credit also revealed improvements for system reliability by co-locating wind and wave energy with generation mixes improving over either resource alone.

Identifying the global optimum generation mix between the system operation metrics and the system reliability metrics likely requires a full hourly simulation of the electric power system and electricity markets with a total cost methodology. With the wide uncertainties of capital costs for offshore wind power in deep water, wave power, and subsea transmission systems, the results of such a study are likely to be inconclusive. The metrics in this study at present, however, indicate that once capital cost uncertainties are reduced with the commercial advancement of the technology over the next 5–10 years, a total system cost model will likely demonstrate generation mixes of wind and wave power superior to either resource alone. This was shown in [16] for the UK.

There are two important limitations to this study. First, the results of this study should be interpreted as an exploration of the synergistic potential of co-locating the two marine renewables in California where their low temporal correlations lead to less
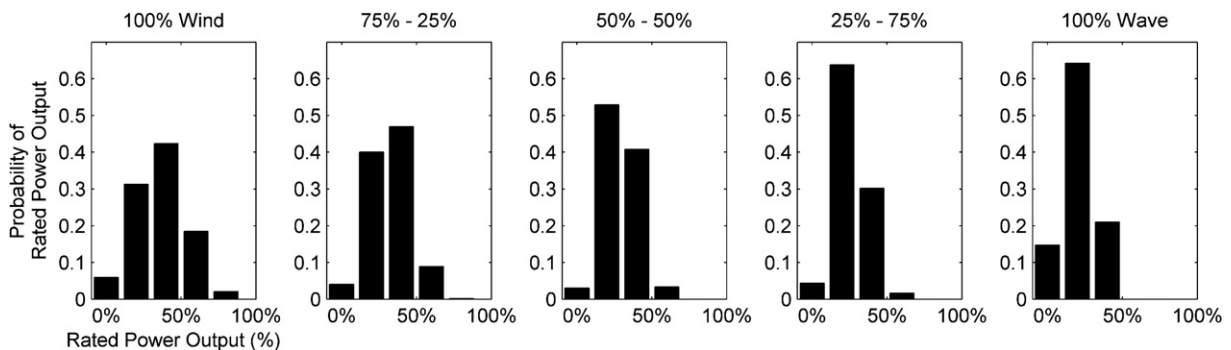

Fig. 12. Probability of the aggregate rated power output state of ten 500 MW wind and/or wave energy farms operating during the summer of 2001.

Table 3
Loss of load expectation (LOLE) and capacity credit for all generation mixes of ten 500 MW farms for the year 2001 in the simplified California generation system model.

	Generation Mix					
	100% gas	100% wind	75%–25%	50%–50%	25%–75%	100% wave
No. of 100 MW gas plants	54	42	42	42	43	46
No. of 200 MW gas plants	185	185	185	185	185	185
Gas Plant (MW)	42,400	41,200	41,200	41,200	41,300	41,600
Wind power (MW)	–	5000	3750	2500	1250	–
Wave power (MW)	–	–	1250	2500	3750	5000
System Capacity (MW)	42,400	46,200	46,200	46,200	46,300	46,600
LOLE (hours/yr)[a]	2.36	2.09	2.02	2.23	2.33	2.39
Capacity Factor	94%[b]	36%	33%	29%	25%	21%
Capacity Credit	–	24%	24%	24%	22%	16%

[a] LOLE requirement < 2.4 h/year (0.1 day/year).
[b] Forced outage rate for CCGT = 6.16% (NERC); Capacity Factor = 1-FOR; excludes scheduled maintenance outages.

variable aggregate power on all time scales. Direct competitive comparisons of the performance of wind and wave power should be avoided and cannot be conclusively drawn from these results as the market and technology cost will ultimately decide this.

The second limitation is this study and the data are not a California resource assessment of offshore wind energy [27,28] and wave energy [31]. The data and model best capture the variable power output characteristics of wind and wave energy and their system impacts rather than identifying the highest resource sites in California because the locations were dependent entirely on the buoy locations. Additionally, the use of one wave energy converter, the Pelamis, reflects the power extraction by that converter and not all wave energy converters in general. However, the variability in power output, the central subject of this study, is likely similar for all wave power converters. Furthermore, no environmental, sea space uses, zoning, permitting, or transmission interconnection issues were considered for the marine renewable energy farms modeled for this study.

4. Conclusion

In this study the extensive data set of 143 annual records of hourly offshore wind and wave measurements maintained by the National Data Buoy Center was used to model the power performance and variability of offshore wind and wave energy farms in California. Methodology and metrics used to quantify wind power performance, variability, and power system integration impacts were extended to wave energy.

At the buoys, offshore wind farms would have capacity factors ranging from 30% to 50%, and wave farms would have capacity factors ranging from 22% to 29%. A correlation matrix was constructed that compares resource diversity with geographic diversity. Aggregate power from a co-located wind and wave farm achieves reductions in variability equivalent to aggregating power from two offshore wind farms approximately 500 km apart or two wave farms approximately 800 km apart. Combined farms in California would have less than 100 h of no power output per year, compared to over 1000 h for offshore wind or over 200 h for wave farms alone. These combined farms of wind and wave would best be located near capes and points along the coast where regions of high wind and wave resources overlap.

Power system operation and reliability metrics were used to assess the impacts of various wind and wave energy farms within a simplified model of the California electric power system. Combining these resources was shown to reduce the impacts on the system from variable power generation. This reduced the requirement for load following reserves and generation capacity to maintain system reliability, which lowers the system integration costs for combined marine renewables compared to either offshore

wind or wave energy alone. Ten offshore farms of wind, wave, or both modeled in the California power system would have capacity factors during the summer of 2001 ranging from 21% (all wave) to 36% (all wind) with combined wind and wave farms between 21% and 36%. The capacity credits for these farms range from 16% to 24% with some combined wind and wave farms achieving capacity credits equal to or greater than a 100% wind farm because of their reduction in power output variability.

Acknowledgements

References

[1] Kahn E. The reliability of distributed wind generators. Electric Power Systems Research 1979;2:1–14.
[2] Milligan M, Artig R. Reliability benefits of dispersed wind resource development. Windpower 1998; April 27-May 1, 1998. Golden, CO: National Renewable Energy Laboratory; 1998.
[3] Milligan M, Artig R. Choosing wind power plant locations and sizes based on electric reliability measures using multiple-year wind speed measurements. US Association for Energy Economics; 1999. August 29-September 1.
[4] Gregor Giebel. On the benefits of distributed generation of wind energy in Europe. Dissertation, Carl von Ossietzky Universitaet Oldenburg; 2000.
[5] Milligan M, Factor T. Optimizing the geographic distribution of wind plants in iowa for maximum economic benefit and reliability. Wind Engineering 2000; 1 July 2000; 24:271–90.
[6] Holttinen H. Hourly wind power variations in the Nordic countries. Wind Energy 2005;8(2):173–95.
[7] Gross R, Heptonstall P, Leach M, Anderson D, Green T, Skea J. Renewables and the grid: understanding intermittency. Proceedings of the Institution of Civil Engineers. Energy 2007;160(1):31–41.
[8] Sinden G. Characteristics of the UK wind resource: long-term patterns and relationship to electricity demand. Energy Policy 2007;35(1):112–27. 1.
[9] Archer CL, Jacobson MZ. Supplying baseload power and reducing transmission requirements by interconnecting wind farms. Journal of Applied Meteorology and Climatology 2007 November;46(11):1701–17.
[10] Beyer HG. Power fluctuations from geographically diverse, grid coupled wind energy conversions systems. In: European wind energy conference proceedings; February 1989. p. 306–10.
[11] Beyer HG, Luther J, Steinberger-Willms R. Power fluctuations in spatially dispersed wind turbine systems. Solar Energy 1993;50(4):297–305.
[12] Nanahara T, Asari M, Maejima T, Sato T, Yamaguchi K, Shibata M. Smoothing effects of distributed wind turbines. Part 2. Coherence among power output of distant wind turbines. Wind Energy 2004;7(2):75–85.
[13] Wan Y, Milligan M, Parsons B. Output power correlation between adjacent wind power plants. Journal of Solar Energy Engineering 2003;125(4):551–5.
[14] Milligan M, Porter K, Parsons B, Caldwell J. wind energy and power system operations: a survey of current research and regulatory actions. The Electricity Journal 2002;15(2):56–67. 3.
[15] Parsons BK, Wan Y, Kirby B. Wind farm power fluctuations, ancillary services, and system operating impact analysis activities in the United States. Golden, CO: National Renewable Energy Laboratory; 2001. Preprint.
[16] Tipping J. The benefits of marine technologies within a diversified renewables mix. Redpoint Energy Ltd.; 2009. Report for BWEA.
[17] Holttinen H. Impact of hourly wind power variations on the system operation in the Nordic countries. Wind Energy 2005;8(2):197–218.

[18] Holttinen H, Milligan M, Kirby B, Acker T, Neimane V, Molinski T. Using standard deviation as a measure of increased operational reserve requirement for wind power. Wind Engineering 2008;32:355–77.

[19] Milligan MR, Artig R. Choosing wind power plant locations and sizes based on electric reliability measures using multiple-year wind speed measurements. Medium, ED Size: vp; 1999.

[20] Milligan MR. A chronological reliability model to assess operating reserve allocation to wind power plants. Golden, CO: National Renewable Energy Laboratory; 2001. Preprint.

[21] Wangdee W, Billinton R. Considering load-carrying capability and wind speed correlation of WECS in generation adequacy assessment. Energy Conversion, IEEE Transactions on 2006;21(3):734–41. 21.

[22] Lund H. Large-scale integration of optimal combinations of PV, wind and wave power into the electricity supply. Renewable Energy 2006;31(4):503–15.

[23] Sinden G. Diversified renewable energy resources. Oxford: The Carbon Trust; 2006.

[24] Stoutenburg ED, Jacobson MZ. Combining wind and wave energy in offshore power plants. San Francisco: American Geophysical Union Fall Meeting; December 15-19, 2008.

[25] Stoutenburg ED, Jacobson MZ. Quantifying the benefits of combining offshore wind and wave energy. San Francisco: American Geophysical Union Fall Meeting; December 14-18, 2009.

[26] Fusco F, Nolan G, Ringwood JV. Variability reduction through optimal combination of wind/wave resources – an Irish case study. Energy 2010;35 (1):314–25.

[27] Jiang Q, Doyle JD, Haack T, Dvorak MJ, Archer CL, Jacobson MZ. Exploring wind energy potential off the California coast. Geophysical Research Letters 2008;35(10/28).

[28] Dvorak MJ, Archer CL, Jacobson MZ. California offshore wind energy potential. Renewable Energy 2010;35(6):1244–54.

[29] StatoilHydro. Hywind. Available at, http://www.statoilhydro.com/en/TechnologyInnovation/NewEnergy/RenewablePowerProduction/Onshore/Pages/Karmoy.aspx; 2009 [accessed 15.09.09].

[30] Jonkman JM. Dynamics of offshore floating wind turbines - model development and verification. Wind Energy 2009;12(5):459–92.

[31] Wilson JH, Beyene A. California wave energy resource evaluation. Journal of Coastal Research 2007;23(3):679–90.

[32] European Marine Energy Centre. Available at, http://www.emec.org.uk/ [accessed 06.11.09].

[33] Pelamis Wave Power Ltd. Pelamis wave energy converter. Available at, http://www.pelamiswave.com/ [accessed 15.09.09].

[34] Billinton R, Allan R. Reliability evaluation of power systems. 2nd ed. New York: Plenum Press; 1996.

[35] Billinton R, Gao Yi. Multistate wind energy conversion system models for adequacy assessment of generating systems incorporating wind energy. Energy Conversion, IEEE Transactions 2008;23(1):163–70.

[36] Gao Y, Billinton R. Adequacy assessment of generating systems containing wind power considering wind speed correlation. Renewable Power Generation, IET 2009;3(2):217–26.

[37] Milligan M, Porter K. Determining the capacity value of wind: an updated survey of methods and implementation. Golden, CO: National Renewable Energy Laboratory; 2008. Preprint.

[38] National Oceanic and Atmospheric Adminstration's National Data Buoy Center. Available at, http://www.ndbc.noaa.gov/.

[39] Handbook of automated data quality control checks and procedures. National Data Buoy Center; 2009. NDBC Technical Document 09-02.

[40] Hsu SA, Meindl EA, Gilhousen DB. Determining the power-law wind-profile exponent under near-neutral stability conditions at sea. Journal of Applied Meteorology 1994;33:757–65.

[41] Capps SB, Zender CS. Global ocean wind power sensitivity to surface layer stability. Geophysical Research Letters 2009;36(05/1).

[42] Nørgård P, Holttinen H. A multi-turbine power curve approach. nordic wind power conference. Chalmers; 1–2 March 2004.

[43] Earle M. Nondirectional and directional wave data analysis procedure. NDBC Technical Document 96–01; 1996.

[44] Previsic M, Bedard R, Hagerman G, Siddiqui O. System level design, performance and costs for san francisco california pelamis offshore wave power plant. Report WP-006-SFa; 2004.

[45] Ochi M. Ocean waves: the stochastic approach. Cambridge: Cambridge University Press; 1998.

[46] Barthelmie R, Larsen G, Pryor S, Jørgensen H, Bergström H, Schlez W, et al. ENDOW (efficient development of offshore wind farms): modelling wake and boundary layer interactions. Wind Energy 2004;7(3):225–45.

[47] Barthelmie RJ, Hansen K, Frandsen ST, Rathmann O, Schepers JG, Schlez W, et al. Modelling and measuring flow and wind turbine wakes in large wind farms offshore. Wind Energy 2009;12(5):431–44.

[48] Cruz J, editor. Ocean wave energy: current status and future prepectives. Berlin Heidelberg: Springer; 2008.

[49] Green J, Bowen A, Fingersh LJ, Wan Y. Electrical collection and transmission systems for offshore wind power. offshore technology conference; 30 April–3 May 2007.

[50] Söder L, Holttinen H. On methodology for modelling wind power impact on power systems. International Journal of Global Energy Issues 2008;29(1/2):181–98.

[51] Brown D. Summer. 2008 electricity supply and demand outlook. CEC-200-2008-003; 2008.

[52] North American Electric Reliability Corp. Generating availability data system. Available at, http://www.nerc.com/page.php?cid=4|43 [accessed 06.11.09].

[53] 2008 summer loads and resources operations preparedness assessment. California Independent System Operator Corporation; 2008.

[54] Oasis: system load reports. California Independent System Operator Corporation. Available at, http://oasishis.caiso.com/; 2009 [accessed 09.11.09].

[55] Dean R, Dalrymple R. Water wave mechanics for engineers and scientists. New Jersey: World Scientific; 2008.

[56] Czisch G, Ernst B. High wind power penetration by the systematic use of smoothing effects within huge catchment areas shown in a European example. Conference paper: AWEA, Washington; 2001.